for pure liquids and dilute solutions," National Bureau of Standards Circular 539, Nov. 1958.
[9] J. Toler and J. Seals, "RF dielectric properties measurement system: Human and animal data," Dept. Health, Education and Welfare (NIOSH) Publication No. 77-176, 1977.

✤

M. A. Stuchly (M'71–SM'76), for a photograph and biography please see page 86 of this issue.

✤

T. Whit Athey, for a photograph and biography please see page 86 of this issue.

✤

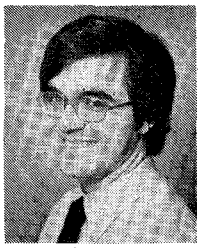

George M. Samaras (S'72–M'76) received the B.S.E.E. (BioMedical) degree, the M.S. degree in physiology, and the Ph.D. degree in neurophysi-ology/neuropharmacology, all from the University of Maryland, College Park, in 1972, 1974, and 1976, respectively. He is an Engineer/Physiologist and an Assistant Professor of Radiology at the University of Maryland School of Medicine, Baltimore. He has extensive experience in computer hardware/software systems interfacing and has worked as a Biomedical Engineer for the Environmental Protection Agency. He is currently doing research and development in microwave-induced hyperthermia systems for use in cancer therapy. He has worked as a Consultant for biomedical and cybernetic system development and was Editor of the *Forum*, a journal of the American Society for Cybernetics.

Dr. Samaras is a member of the AAAS and the AAMI (High Frequency Therapeutic Device Standards Committee).

✤

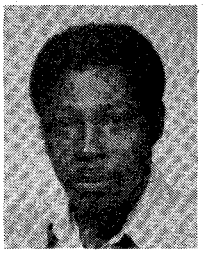

Glen Edward Taylor was born in Baltimore, MD, in 1946. He graduated from the Community College of Baltimore, Baltimore, MD.

From 1968 to 1973 he worked for the National Pituitary Agency, and from 1973 to 1979 he worked for the Department of Pediatrics Research, both at the University of Maryland, Baltimore. Since 1979 he has worked for the Department of Radiation Therepy at the University of Maryland Hospital. His field of Research is in Biochemistry.

Waveguide Technique for the Calibration of Miniature Implantable Electric-Field Probes for Use in Microwave-Bioeffects Studies

DOUGLAS A. HILL

Abstract—**A new S-band waveguide technique has been developed for the calibration of miniature probes used in determining electric fields in biological tissues at 2.45 GHz. A section of waveguide is filled with tissue-equivalent liquid separated from the air-filled waveguide by a very thin (0.25-mm) planar dielectric spacer. The probe response is measured as a function of position on each side of the spacer and extrapolated to the interface. The ratio of probe response in air to that in test liquid is then determined assuming continuity of tangential E-field across the spacer. In the water–glycerol solution modelling wet tissue, the probes are 3.0 ± 0.6 times more sensitive to E^2 than in air. A wide variety of both wet and dry tissues may be simulated using liquids of different dielectric properties—a check on the properties is provided by comparing the measured depth of penetration of the wave in the liquid with the calculated value. Problems using the probes in biological tissues are also discussed.**

Manuscript received March 23, 1981; revised July 30, 1981. This work was performed at the Division of Biological Sciences, National Research Council, Ottawa, and issued as DREO Report No. 847.

The author is with the Radiation Biology Section, Protective Sciences Division, Defence Research Establishment Ottawa, Department of National Defence, Ottawa, Canada K1A 0Z4.

I. Introduction

FOR MICROWAVE bioeffects research it is desirable to know the *local* rate of energy deposition at the site of action of the microwave radiation. The rate of energy deposition is usually expressed as a specific absorption rate

0018-9480/82/0100-0092$00.75 ©1982 IEEE

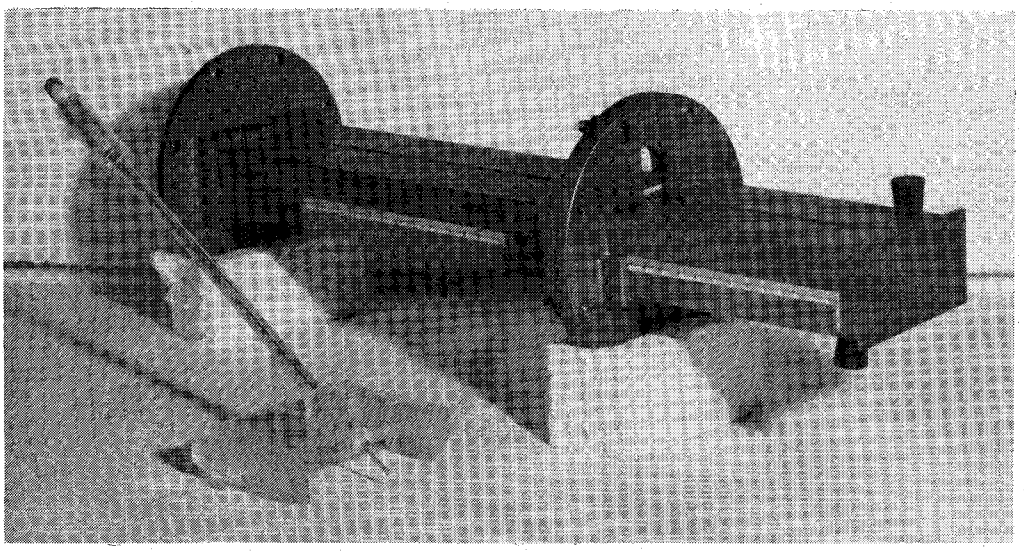

Fig. 1. Photo of a miniature electric-field probe in the probe holder used for both waveguide and anechoic-chamber calibration measurements. The slotted waveguide assembly, used for determining probe response in liquids, is filled with air to the left of the center flange and test liquid to the right.

(SAR) (watts/kilogram), and is known from the basic physics to be given by

$$\text{SAR} = (\sigma/\rho)E_T^2 \qquad (1)$$

where σ is the electrical conductivity, in siemens/meter, ρ is the density (kilograms/cubic meter) of the medium, and E_T is the total electric field strength (rms V/m) in the medium. When σ and ρ are known quantities, a measure of E_T^2 in the medium gives the SAR.

Three different groups (led by Bassen [1], [2], Chen [3], [4], and Smith [5], [6]) have fabricated miniature probes which measure E_T^2 in microwave-exposed tissues or tissue-equivalent materials. In addition, some of them [4]–[6] have calculated the response of bare and insulated antennas in tissue-equivalent media at radio or microwave frequencies. Two methods of calibrating these probes have been reported where tissue-equivalent material, in the form of a semi-infinite slab [7] or sphere [1], [2], is exposed in an anechoic chamber. This paper reports a new waveguide technique for the calibration of these probes for use both in air and in tissue at 2.45 GHz.

II. Probes

A. Design

The probes used were produced in 1978 as Narda Microwave Corporation Model #25256 (prototype) following Bassen's "BRH model 10" design [2]. One of the probes is shown in Fig. 1 and details of the miniature dipole antenna design in the tip are given in Fig. 2. The antenna is encased in a 1.2-mm-thick 2.3-mm-wide planar dielectric substrate of dielectric constant $\simeq 2$. The high-resistance lines carry the rectified dipole voltage to a digital dc voltmeter without any microwave pickup. The 55° offset angle of dipole with respect to the long probe axis allows the single dipole to be

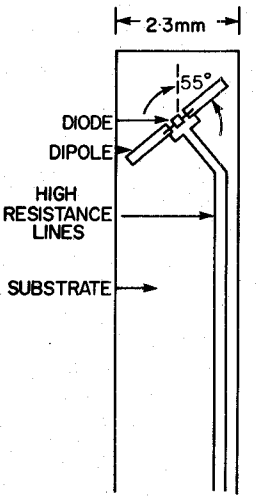

Fig. 2. Design details for the miniature dipole antenna structure in the probe tip (from Bassen *et al.* [2], with permission).

oriented in three mutually perpendicular directions by successive rotations of the probe about its axis by 120°.

The evaluation of the performance and utility of this particular prototype probe design has been reported in detail by Hill and Hartsgrove [8]. Briefly, we encountered two problems with the probes.

1) Several of them open-circuited after a few days of use with a solid-state electrometer, of very high input impedance, but the problem did not occur with a battery-operated digital voltmeter of 10^{10}-Ω input impedance. The latter was therefore used in all tests reported here.

2) The problem of a mechanical weakness at the joint near the tip was reduced by strengthening the joint with epoxy glue and using the probes with care. Nevertheless, several probes broke during use so the data in the two tables are not quite complete. A new version of the probe,

incorporating an epoxy-fiberglass tip, has eliminated the breakage problem [9].

B. Definition of Response Coefficients

The probe output voltage V_i for probe orientation number i ($i=1,2,3$) is proportional to the square of the electric field-strength E_i along the dipole axis for that orientation

$$V_i = B_M E_i^2 \tag{2}$$

where B_M is an empirical constant depending on the medium and also slightly on E_i (or V_i). The value of B_M for air is designated B_A.

Summing the three perpendicular components of (2) gives the relationship between the total voltage V_T and the total electric field E_T

$$V_T = V_1 + V_2 + V_3 = B_M E_T^2. \tag{3}$$

Since the probe is also used to measure the power density in free space P_D related to E_T by

$$P_D = E_T^2/377 \tag{4}$$

(3) may also be written as

$$V_T = C_A P_D \tag{5}$$

where C_A depends slightly on the value of P_D (or V_T). The air response will be discussed primarily in terms of C_A while B_M will be used for measurements in other media.

III. Probe Calibration in Air

A. Waveguide Technique

To calibrate the probe response in air, the measurement system of Fig. 3 is used with the matched load as the final component. The probe tip is put into the center of the slotted waveguide and the probe voltage V_T is measured as a function of net forward power in the waveguide P_0. The latter is then related to E_T^2 by the equation developed in the Appendix, and B_A or C_A is determined from (3) or (5), respectively.

The microwave frequency is determined with a calibrated coaxial transmission wavemeter. The VSWR of either test cell or matched load (VSWR$<$1.04) is measured with the commercial slotted line. The probe under test is shown in its holder in Figs. 1 and 3. The 55° angle built into the holder allows the rotation of the probe to the position of maximum response where the dipole is parallel, within $\pm 5°$, to the (vertical) electric field in the waveguide. The voltage reading in this one position V_1 must be corrected slightly for the other two components, V_2 and V_3, which are nonzero because of possible probe misalignment and/or anisotropic response. Thus V_T is measured to be $(1.07 \pm 0.02)V_1$. P_0 is determined from the forward and reflected power measurements in the coaxial part of the system, neglecting any loss in the coax-to-waveguide adapter. The total error in the determination of C_A is estimated to be ± 9 percent.

A typical calibration curve of V_T versus P_D is shown in Fig. 4. The value of C_A ($\simeq 1$ mV/mW$\cdot$cm^{-2}) in (5) can be read off the curve at different values of P_D. On the log–log plot shown, the points lie on a straight line from about 0.5 to 15 mW$\cdot$cm^{-2} with a slope of 0.96 ± 0.02, which is close to unity.

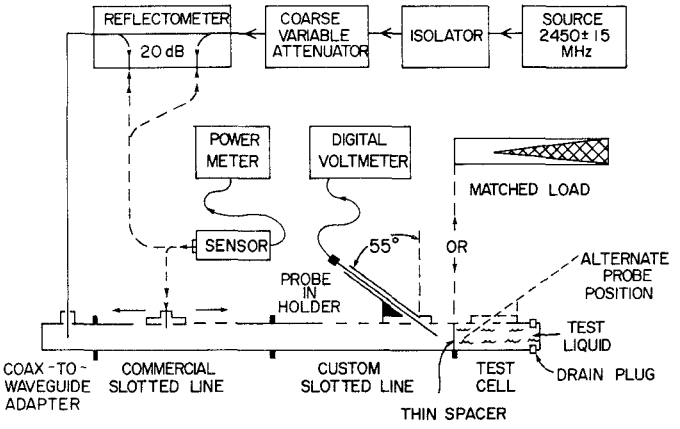

Fig. 3. Hybrid coaxial-waveguide system for probe calibration measurements in air (using the matched load), or in test liquids (using the test cell).

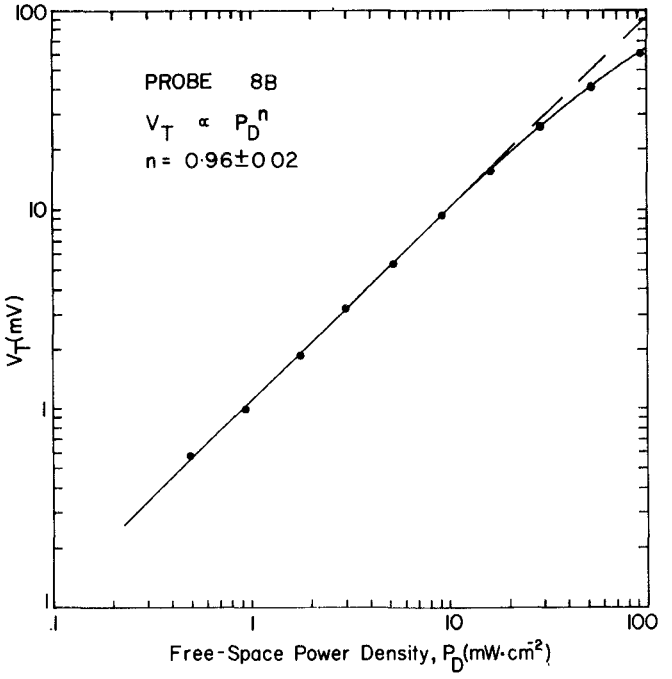

Fig. 4. Calibration curve for the use of probe 8B in air.

B. Comparison with Other Techniques

Most of the probes were supplied from Narda Microwave with a C_A value determined at power densities of 1 and 10 mW$\cdot$cm^{-2}. Their method involved inserting the probe through a small hole in the narrow side of S-band waveguide and positioning it so that the dipole sensed the full electric field at the center of the waveguide.

In addition, two probes were also calibrated in our anechoic chamber [10]. It was found convenient to use the probe in the same holder on a large block of polystyrene

TABLE I
SUMMARY OF PROBE CALIBRATION DATA FOR AIR

Probe Serial Number	Power-Law Slope (n)	C_A (mV/mW·cm^{-2}) at a Power Density of: 1 (mW·cm^{-2})	10			50	
		(a)	(a)	(b)	(c)	(a)	(b)
5	0.95	1.20	1.07		1.06		
6	0.94	1.17	1.01		1.04		
7B	0.92	1.31	1.10	1.27 ± 0.23		0.88	0.87 ± 0.16
8B	0.96	1.10	1.00	0.91 ± 0.16	1.29	0.80	0.78 ± 0.14
9	0.96	0.89	0.82		0.96		
mean	0.95	1.13	1.00	1.09	1.09	0.84	0.83
± SE	± 0.02	± 0.07	± 0.05		± 0.07		

(a) our waveguide data; (b) our anechoic-chamber data;
(c) Narda Microwave waveguide data.

foam, although this caused a small (±6-percent) error due to the measured interference of the lucite probe holder [8]. The exposure power density was determined using either of two Narda Microwave model 8305 radiation monitors or a Holaday Industries model HI 1500 microwave survey meter, which all agreed within 5 percent. Allowing for the ±12-percent (±0.5-dB) error in power-density probes and the ±6-percent error above, the total uncertainty in determining C_A from anechoic-chamber measurements was about ±18 percent.

The data from the three different air-calibration procedures are summarized in Table I, where they can be seen to be in excellent agreement within the estimated uncertainties.

IV. Probe Calibration in Tissue-Equivalent Liquids

A. Introduction

The probes produce a larger output voltage for the same E^2 exposure in any medium of dielectric constant $\epsilon' > 1$, than for air, i.e., $B_M(\epsilon') > B_A$. To evaluate $B_M(\epsilon')$, the end section of waveguide shown in Fig. 3 is filled with different test liquids having a range of ϵ' values chosen to span those of both wet and dry biological tissues. The liquid-filled waveguide is separated from the air-filled waveguide by a thin plastic planar spacer inserted between the waveguide flanges. In the air-filled waveguide the electric field of the TE_{10} mode is tangential to the surface of the spacer. This tangential field is denoted as E_t(air). For our standard probe orientation, the sensing dipole is parallel to E_t and the output voltage V_1 is given by (2), i.e.,

$$V_1(\text{air}) = B_A E_t^2(\text{air}). \tag{6}$$

Similarly, the response in the liquid is given by

$$V_1(\text{liquid}) = B_M(\epsilon') E_t^2(\text{liquid}). \tag{7}$$

Using the boundary condition that the tangential component of E is continuous across any interface, and ignoring (for the moment) any change in E_t within the thin spacer, we have

$$E_t(\text{liquid}) = E_t(\text{air}). \tag{8}$$

Using (8) to eliminate E_t in (6) and (7) we get

$$\frac{B_M(\epsilon')}{B_A} = \frac{V_1(\text{liquid, at interface})}{V_1(\text{air, at interface})}. \tag{9}$$

By measuring V_1 as a function of position on each side of the spacer and extrapolating the curves up to the interface, the ratio of probe response coefficients, B_M/B_A, can be determined using (9). Care must be taken in determining the distance of the probe dipole from the spacer and in assuring that the test cell (and a bit of the slot) is completely filled with liquid.

It is well known that the electric field inside a lossy test liquid decays exponentially. The squared electric field, proportional to power, also decays exponentially with the form

$$E^2(x) = E^2(0)\exp(-x/\delta_2) \tag{10}$$

where x is the distance into the liquid from the interface and δ_2 is the characteristic penetration depth for power. Since $V_1(x)$ is a measure of $E^2(x)$, δ_2 can be determined directly from the graph of $V_1(x)$ in the liquid.

B. Measurements

Typical results for $V_1(x)$ measured on both sides of the interface are shown in Fig. 5. To account for the effect of the spacer and minimize the error due to probe-position uncertainty, the curves (a) for air were shifted (by no more than 0.4 mm) along the position axis to give the best-fit single curve through all the data points on both sides of the interface. This procedure reduced the position uncertainty to ±0.2 mm on each side of the interface.

The pairs of curves (b), (c), and (d) show clearly the increased probe response in test liquids. They also demonstrate the exponential decay of the voltages in the test liquids, which are straight lines on the semilogarithmic plot. The sample length in the test cell, 15 cm, is essentially infinite. The curved lines on the air side of the interface show the standing-wave pattern created by the reflection from the liquid.

The ratio B_M/B_A, typically 2.2 to 3.0, is taken from the curves extrapolated to the line representing the center of the thin spacer. There are two main sources of error in this procedure: one due to the ±0.2-mm residual uncertainty in probe position and the other due to the curve-extrapolation process on the air side. The combined uncertainty in the determination of B_M/B_A resulting from these two errors is estimated to range from 0.2 to 0.6 (8 to 25 percent). Approximately 2/3 of the error comes from curve extrapolation which in turn depends on curve shape and slope. The worst case, ±0.6, applies to the water–glycerol solution which simulates wet tissue.

δ_2 is determined directly from the curves in liquid and has an estimated uncertainty of ±10 percent for a single

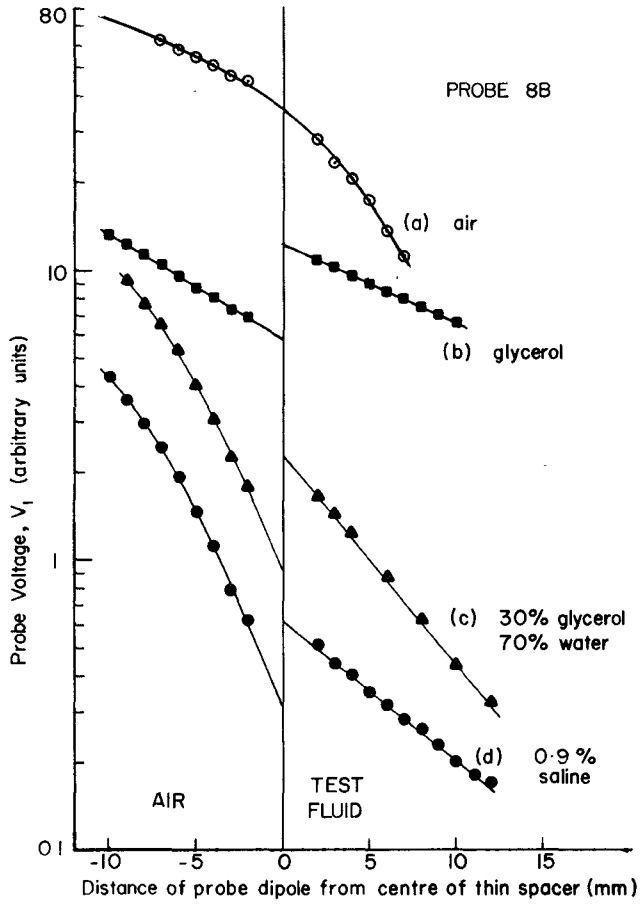

Fig. 5. Probe voltage versus position on both sides of a thin (0.25 mm) spacer separating air from four different test fluids. Each *pair* of corresponding curves has been shifted somewhat along the arbitrary voltage scale to clearly separate them from the other curves.

TABLE II
PROBE RESPONSE RATIO AND POWER PENETRATION DEPTH AT 2.45 GHz IN FOUR DIFFERENT LIQUID DIELECTRICS

Test Liquid	Dielectric Properties: T (°C)	ε'	σ§ (S/m)	Ref. No.	Probe Response Ratio, B_M/B_A: Probe Number 5	6	7B	8B	Mean ± SE	Penetration Depth, δ_2 (mm): Measured (mean ± SE)	Calculated (TE_{10} mode)
glycerol	23	6.3 ± 0.3	0.49 ± 0.05	11	2.9	3.0	2.6	2.2	2.68 ± 0.18	12.9 ± 1.4	13.4 ± 1.2
water:glycerol (70:30 v/v solution)	23	58.5 ± 1.0	2.66 ± 0.20	11	3.0	3.9 2.9	2.8 3.3	2.5 2.6	3.00 ± 0.18	7.7 ± 0.4	7.7 ± 0.6
0.9% (w/w) saline	23	74.3	2.79	12 ¶	2.5	2.5	2.3	2.0 1.8	2.22 ± 0.14	8.3 ± 0.2	8.2
water	20	78.4	1.47	13	3.0	2.2 2.6	1.9	1.8	2.30 ± 0.22	14.3 ± 0.9	16.0
	25	77.2	1.29	13							18.1
Probe Average (mean ± SE)					2.85 ± 0.12	2.85 ± 0.24	2.58 ± 0.24	2.15 ± 0.14	2.59 ± 0.11	← Grand Average (all probes and liquids) (N = 21)	

§ $\varepsilon'' = 7.34\,\sigma$ at 2.45 GHz

¶ The dielectric properties from this reference are for mammalian Ringer solution.

The dielectric properties of wet and dry biological tissues are:

$\varepsilon' = 47$, $\sigma = 2.21$ S/m and $\varepsilon' = 5.5$, $\sigma = 0.1$–0.2 S/m, respectively [14].

determination. The effect of spacer thickness on the measured quantities B_M/B_A and δ_2 was tested. There was no detectable difference between the results using a spacer 0.25 mm thick and those using a 1.37-mm-thick spacer. A spacer thickness of 3.0 mm altered the results. The thinnest spacer (0.25 mm) was used for all data reported here.

The results of all measurements performed on four probes using four test liquids are presented in Table II. All tests were done at room temperature, 19°–22°C.

C. Discussion

The dielectric properties of the four test liquids used are given in Table II along with those of wet and dry tissue for comparison. Glycerol can be seen to approximate dry tissue while the water–glycerol solution is closest to wet tissue. The 0.9-percent saline solution represents body fluids such as blood plasma and cerebro–spinal fluid. Water was also used for comparison since its dielectric properties are precisely known.

The B_M/B_A ratios are reproducible within the estimated uncertainty of ± 0.2 to 0.6 for individual determinations. The average response ratio has been tabulated for each test liquid and each probe. It can be seen that there are real differences between the liquids. In addition, probe 8B, used by Cairnie *et al.* [15] for mouse-tissue measurements, has a response different from the other three probes. For that probe, the response ratio in wet tissue is taken to be 2.5 ± 0.5, based on the water–glycerol results and the estimated measurement uncertainties.

The dependence of the probe response ratio on dielectric constant and conductivity can be seen in Table II. The probes have a slightly lower response in the high-dielectric-constant liquids than in the lower two. This is contrary to the published curves of Smith [5], which were calculated for a small cylindrical dipole surrounded by a cylinder of insulator, and of Mousavinezhad *et al.* [4] for a dual-hemisphere dipole surrounded by a sphere of insulator. This probe's design differs from theirs, being a small planar gold-foil dipole surrounded by a rectangular planar insulator.

My results are almost in agreement with their results for "sufficiently thick" insulation, which show that for all $\epsilon' > 6$ to 10 the response is nearly independent of ϵ'. I found a slightly larger (20–35-percent $\pm$ 15-percent) response in the two liquids of lower ϵ'. In view of the moderate increase involved and the difference in probe geometries, the disagreement between my results and the two calculations is not considered important. The fact that the response ratio is nearly independent of ϵ' permits a probe calibrated in one wet material to be used in other types of soft wet or dry tissue as long as ϵ' is known to be greater than 6.

Bassen *et al.* [2] recently found a probe response ratio of 3.5 for simulated brain material and 5.4 for simulated muscle material for a similar probe used at 2.45 GHz. They also reported a lower response ratio for materials with a lower ϵ' value. As the probe construction was not identical and the dielectric properties have not yet been published, no exact comparison can be made.

The average measured value of δ_2 for each liquid is also presented in Table II. Only the average for all probes is shown since δ_2 was found to be independent of probe number. The propagating mode in the liquid is assumed to be primarily the TE_{10} mode since only that mode can match the boundary conditions at the interface. Table II also gives the value of δ_2 calculated for the TE_{10} mode using the listed dielectric properties and equations (7-38) and (11-1) of Moreno [16]. The comparison of calculated and measured δ_2 values provides a useful check on the measured (or assumed) dielectric properties. For example, this comparison resulted in Brady *et al.* [11] remeasuring the glycerol and water–glycerol solutions for the present author.

The calculated values agree with the measured for all liquids except possibly water. The water was used at room temperature, 20.5 ± 1.5°C, so that temperature variations may account for some of the difference. It can be seen in Table II that δ_2 changes at a rate of 0.4 mm/C°. Another explanation for the discrepancy would be the possible presence of propagating higher order modes. The first higher order mode likely to propagate, based on some similarity to the TE_{10} pattern, is the TE_{30} mode. For water at 20°C, $\delta_2(TE_{30})$ is calculated to be 15.4 mm, in better agreement with the measured value. For the other three solutions the calculated $\delta_2(TE_{30})$ values are: 7.1 mm for glycerol; 7.3 mm for the water–glycerol solution; and 7.9 mm for the saline. These are further from the measured values, especially for glycerol, where the TE_{30} mode can definitely be ruled out. For the other three liquids, the propagating mode cannot be proven to be the TE_{10} mode from δ_2 measurements alone, since the calculated values of the different modes are so closely spaced, and depend so much on temperature. Note, however, that the determination of B_M/B_A does *not* depend on identifying the propagating mode in the liquid.

Finally, it is interesting to note that the curves in solution show no alteration in probe response when the insulated dipole approaches as close as 1.7 mm to the air–solution interface. This is in agreement with Smith's [6] calculations for an insulated cylindrical probe. Using his notation and the worst case—the liquid of lowest ϵ', i.e., glycerol—we have $S/\lambda(\text{in medium}) = 1.7 \text{ mm}/49 \text{ mm} = 0.035$. Using [6, fig. 12] to *estimate* our probe error we get a value of only ± 2 percent, which would be undetectable in our measurements.

V. Measurements in Tissue

A. Theory

With the probe immersed in tissue the voltages from each of the three probe orientations are measured and summed to give V_T. E_T^2 is then determined from the measured V_T and the known calibration constants C_A and (B_M/B_A) using

$$E_T^2 = \left(\frac{3770}{C_A}\right)\left(\frac{B_M}{B_A}\right)^{-1} V_T \tag{11}$$

derived from (3) to (5). The factor of 3770 results from the use of the practical units: $\text{mV/mW} \cdot \text{cm}^{-2}$ for C_A; millivolts for V_T; and volts/meter for E_T.

If the SAR is desired it is determined from (1). The total uncertainty in SAR is about ± 30 to 40 percent, based on

TABLE III
COMPARISON OF THREE TECHNIQUES FOR CALIBRATING PROBE RESPONSE IN TISSUE-EQUIVALENT MATERIALS AT 2.45 GHz

Method:	I	II	III
Author [Reference]	Bassen et al. [2]	Cheung [7]	Hill [This paper]
Exposure facility	anechoic chamber		WR-284 waveguide
Test object	sphere in styrofoam	semi-infinite slab behind a:	
		¼λ-thick matching plate	thin dielectric spacer
Tissue-equivalent material	semi-soft mixture		liquid
Tissue types simulated	wet (e.g. brain or muscle)		wet/dry (e.g. fat)
Dielectric properties			
- range of ε'	only higher values (e.g. 50)		6 to 79
- checked in method?	no (measured separately)	yes (from comparing measured & calc. δ_2 values)	
Electric fields			
- pattern in material	complex multipeak	simple exponential decay	
- determination of calibration field-strength	average fit of several peaks to computer-calculated pattern*	calculated from incident & reflected waves in air	from continuity of extrapolated E_t curves in air & medium

*The calculation of the sphere pattern is very sensitive to small changes in ε' & σ.

the estimated errors of ±20 percent in (B_M/B_A), ±9 percent in C_A, ±10 percent in σ, and ±5 percent in ρ. This assumes perfect contact between probe and tissue.

B. Practice

In another paper [15] we reported the results of a complete dosimetry study of mice exposed to 2.45-GHz radiation under far-field conditions in an anechoic chamber. That study included internal electric-field measurements in the testis and abdomen of 13 mice in 5 different orientations. The scatter in the measurements was large. Two possible reasons for this were: 1) the tissue was found to move and change shape as the *planar* probe tip was rotated, causing the degree of contact between probe and tissue to vary; small air pockets near the probe were hard to eliminate; 2) the 2.6-mm-diameter probe tip was too large for use in a 4×4×6-mm testicle. The repeated insertion and rotation of the probe tended to destroy the tissue.

VI. SUMMARY AND DISCUSSION

A. Technique

The waveguide method for probe calibration in air is more convenient than an anechoic-chamber technique. The relationship of the electric field at the center of the waveguide to the forward power has been developed in the Appendix. The derivation takes into account the difference in wave impedance between the TE_{10} mode in the guide and a plane wave in free space. The results of probe calibrations in air performed in three different ways by two groups agreed within the experimental errors.

The technique for probe calibration in tissue-equivalent liquids determines the probe response ratio B_M/B_A by a method based on the continuity of tangential electric field at an interface. Spacer thickness, if less than 1 mm, has no effect on the results. The method is well-suited to studying probe response as a function of the dielectric properties of the tissue-equivalent liquids. Both wet and dry tissues may be simulated.

Two other probe-calibration techniques have been reported ([2], [7]). Both involved the exposure of a test object of tissue-equivalent material in an anechoic chamber. All three procedures are compared in Table III. It can be seen that method II has some features of each of the other two. The uncertainty in the tissue-calibration constant (B_M) has been carefully estimated at ±30 percent for method III. The accuracy is likely similar for method II and poorer for method I. Method III is limited to the frequency range of the waveguide used. Overall, methods II and III seem comparable to each other and superior to method I in terms of simplicity, utility, and reliability.

B. Results

The probe response in air is about 1 $mV/mW \cdot cm^{-2}$. In glycerol ($\epsilon' = 6.3$), the liquid simulating dry tissue, the probe response is increased by a factor of 2.7±0.5 (average of four probes). For the water–glycerol solution ($\epsilon' = 58.5$) simulating wet tissue, the increase is 3.0±0.6. The fact that the enhanced sensitivity is nearly independent of dielectric constant is very convenient for its use in tissue.

There was no change in probe response when the probe was brought as close as 1.7 mm to an air–liquid interface, in agreement with the calculations.

Cairnie *et al.* [15] have used the probes for tissue electric-field measurements in mouse abdomen and testis. Although useful results were obtained, there was a large scatter in the data and difficulties were encountered in using the probes. They concluded that the 2.6-mm-diameter planar probe tip is the wrong shape for rotation in tissue and is too large for use in a small-diameter organ such as a

mouse testicle. Bassen *et al.* [1] used a similar probe for *in vivo* field-strength measurements in a larger organ, a cat's brain, and did not report any problems.

APPENDIX

Waveguide Power Density and Electric Field

At the center of an air-filled rectangular waveguide propagating the usual TE_{10} mode the electric field only has one component, parallel to the short face of the guide and perpendicular to the broad face. This one component will be denoted E_T since it is the total field. The magnetic field also has only one component H_T. By definition, the power density P_D' is $E_T \cdot H_T$; the wave impedance, Z, is E_T/H_T; and so $E_T^2 = P_D' \cdot Z$. Expressions for P_D' and Z have been developed by Larsen [17] and by Hill and Hartsgrove [8] using standard waveguide equations (e.g., [16, eqs. (3-3), (7-1)–(7-4), and (7-44)]. The expressions are (1) $P_D' = (2P_0/ab)$, where P_0 is the net forward power in the waveguide, of dimensions $a \times b$; (2) $Z = Z_0(\lambda_g/\lambda)$, where Z_0 is the characteristic wave impedance of free space (377 Ω) and λ and λ_g are the free-space and guide wavelengths, respectively. From the above, one has

$$E_T^2 = \left(\frac{2Z_0}{ab}\right)\left(\frac{\lambda_g}{\lambda}\right)P_0.$$

The probe is also used to measure the power density in free space, $P_D = E_T^2/377$, which differs from P_D' by the ratio (λ_g/λ).

As an example, for the case of a forward power of $P_0 = 1$ W, at a frequency of 2.45 GHz, in *S*-band waveguide (WR-284), we have $a = 7.214$ cm, $b = 3.40$ cm, $\lambda = 12.24$ cm, $\lambda_g = 23.09$ cm, $Z = 713$ Ω, $E_T = 762$ V/m (rms) $P_D' = 81.6$ mW·cm^{-2}, and $P_D = 154$ mW·cm^{-2}.

ACKNOWLEDGMENT

The technical assistance of G. Hartsgrove throughout this work is greatly appreciated.

The author would like to thank H. Bassen of the (U.S.) Bureau of Radiological Health and E. Aslan of Narda Microwave Corporation for their helpful advice and discussions on the design and use of the probes. In addition, the author thanks Bassen *et al.* for permission to use one figure from their draft evaluation report [2].

The author is also grateful to the group at the University of Ottawa for permission to use their unpublished dielectric measurements [11] for glycerol and the water–glycerol solution at 2.45 GHz.

REFERENCES

[1] H. Bassen, P. Herchenroeder, A. Cheung, and S. Neuder, "Evaluation of an implantable electric-field probe within finite simulated tissues," *Radio Science*, vol. 12, no. 6(S), pp. 15S–25S, Nov.–Dec. 1977.

[2] H. Bassen, K. Franke, T. W. Athey, and E. Aslan, "An improved implantable electric field probe," (U.S.) Bureau of Radiological Health, BRH draft internal report, 1981.

[3] B. S. Guru and K.-M. Chen, "Experimental and theoretical studies on electromagnetic fields induced inside finite biological bodies," *IEEE Trans. Microwave Theory Tech.*, vol. MTT-24, pp. 433–440, July 1976.

[4] S. H. Mousavinezhad, K.-M. Chen, and D. P. Nyquist, "Response of insulated electric field probes in finite heterogeneous biological bodies," *IEEE Trans. Microwave Theory Tech.* vol. MTT-26, pp. 599–607, Aug. 1978.

[5] G. S. Smith, "A comparison of electrically short bare and insulated probes for measuring the local radio frequency electric field in biological systems," *IEEE Trans. Biomed. Eng.*, vol. BME-22, pp. 477–483, Nov. 1975.

[6] G. S. Smith, "The electric-field probe near a material interface with application to the probing of fields in biological bodies," *IEEE Trans. Microwave Theory Tech.*, vol. MTT-27, pp. 270–278, Mar. 1979.

[7] A. Y. Cheung, "Electric field measurements within biological media," in *Proc. Conf. Biological Effects Measurement Radio Frequency/Microwaves*, (Rockville, MD) HEW Publication (FDA) 77-8026, July 1977, pp. 117–135.

[8] D. A. Hill and G. W. Hartsgrove, "Technique for calibrating miniature electric-field probes for use in microwave bioeffects studies at 2450 MHz: evaluation and calibration of BRH-Narda probes," Defence Research Establishment Ottawa, Canada, Technical note 80-31, Oct. 1980 (available from Defence Scientific Information Service, National Defence Headquarters, Ottawa, Canada, K1A 0Z4).

[9] H. Bassen, Bureau of Radiological Health, private communication, Sept. 1980.

[10] H. M. Assenheim and G. W. Hartsgrove, "The design and evaluation of an anechoic chamber for the irradiation of small and large animals," National Research Council of Canada, Report no. 17448.

[11] M. Brady, G. Gajda, A. Thansandote, and S. S. Stuchly, Dep. Electrical Engineering, University of Ottawa, Ottawa, Canada, private communication, Sept. 1980, (preliminary measurements of the dielectric properties of glycerol and water–glycerol solutions using a new probe technique).

[12] C. K. Chou and A. W. Guy, "Effects of electromagnetic fields on isolated nerve and muscle preparations," *IEEE Trans. Microwave Theory Tech.*, vol. MTT-26, pp. 141–147, Mar. 1978.

[13] J. B. Hasted, *Aqueous Dielectrics*, 1st ed. London: Chapman and Hall, 1973, pp. 43–45.

[14] C. C. Johnson and A. W. Guy, "Nonionizing electromagnetic wave effects in biological materials and systems," *Proc. IEEE*, vol. 60, pp. 692–718, June 1972.

[15] A. B. Cairnie, D. A. Hill, and H. M. Assenheim, "Dosimetry for a study of effects of 2.45-GHz microwaves on mouse testis," *Bioelectromagnetics*, vol. 1, pp. 325–336, 1980.

[16] T. Moreno, *Microwave Transmission Design Data*, 1st ed. New York: McGraw-Hill, 1948, (reprinted by Dover in 1958).

[17] E. B. Larsen, "Techniques for producing standard EM fields from 10 kHz to 10 GHz for evaluating radiation monitors," in *Electromagnetic Fields in Biological Systems*, (IMPI Publication 78CH1438-1 MTT), 1979, pp. 96–112.

Douglas A. Hill received the B.Sc. (honours) degree in mathematics and physics from the University of Toronto, Toronto, Canada, in 1966. He then received the Ph.D. degree in physics at the University of British Columbia, studying microwave cyclotron resonance in p-type GaSb at 35 GHz. From 1972 to 1974 he held a Medical Research Council of Canada Fellowship in the Department of Biophysics at the University of Western Ontario, studying nerve biophysics.

He is now with the Radiation Biology Section of the Defence Research Establishment Ottawa, working in a joint group with the National Research Council of Canada studying the biological effects of radiofrequency and microwave radiation. He is primarily involved in bioeffects dosimetry studies. His main project is the first measurement of whole-body RF absorption in human subjects.